Testing theories of gravitation with the Interstellar Probe Radio Experiment

Michael Plumaris[a], Fabrizio De Marchi[a], Gael Cascioli[b,c], Luciano Iess[a]

[a] *Department of Mechanical and Aerospace Engineering, Sapienza University of Rome, 00184, Italy*
[b] *Center for Space Sciences and Technology, University of Maryland Baltimore County, MD 21250, USA*
[c] *NASA Goddard Space Flight Center, MD 20771, USA*

Abstract

General Relativity (GR) will soon celebrate its 110th birthday, holding up against all experimental enquiry. Nonetheless, unification theories attempting to quantize gravity, such as string theory, are gaining footing. These hypothesize additional scalar, vector, and tensor long-range fields that couple to matter [1], introducing violations to GR. Although such violations have never been detected, it is likely that GR will not be the ultimate theory of gravity. What is certain is that gravity tests are alive and well, pushing the validity of GR to new scales and accuracies, or -potentially- suggesting alternative routes for new physics.

Building upon the legacy of Voyager and Pioneer missions, which demonstrated the capability to survive in the outer reaches of the solar system, the Interstellar Probe mission concept [2] aims to characterise our heliosphere through state-of-the-art instrumentation, opening new frontiers also for GR testing. In this work, we investigate the possibility of constraining the Nordtvedt parameter η and the mass of the graviton via the Compton wavelength λ_C, by simulating the processing of 10 years of radiometric data from the Interstellar Probe. Station calibration and clock synchronisation, as well as limiting spacecraft precession manoeuvres are highlighted as key strategies for obtaining high-quality estimates. In the most favourable scenario, η can be constrained to less than $1.5 \cdot 10^{-5}$, reducing the uncertainty obtained via Lunar Laser Ranging [3], and a lower bound of $1.4 \cdot 10^{14}$ km is set for λ_C, improving the estimates obtained from planetary ephemerides [4] and gravitational wave detection [5]. Extending ranging measurement acquisition to 20 years improves the results tenfold. This experiment interrogates fundamental physics from an unique dynamical setting, investigating possible violations of the Equivalence Principle (EP) underlying GR.

1. Introduction

Although Einstein's Equivalence Principle (EP) underlies General Relativity (GR), there are no strong theoretical reasons to expect this principle to be valid in nature, suggesting that GR should be replaced by a more inclusive theory of gravity [6]. In fact, many theories support a violation of the EP at some level, both from the effects of quantum gravity and those deriving from string theory [1]. This motivates conducting tests of GR, the EP, and the gravitational $1/r^2$ law, in an effort to search for new interactions.

Exposure to large gravitational potentials and the accompanying velocity variations have endowed spacecraft with wide signals for testing fundamental theories of gravity, exploited via atomic clocks, interferometers and Lunar Laser Ranging (LLR) experiments (consult [1] for a complete overview). On astronomical scales, experiments have been conducted, such as gravitational-wave detection [7], which show consistency with GR predictions. Yet, at intermediate scales (10-1000 AU, see Figure 1) gravity has never been accurately tested. Closing this gap is within the performances of modern radiometric techniques and instrumentations, which are capable of unprecedented measurement accuracies, such as the cm-level ranging accuracy demonstrated by BepiColombo [8].

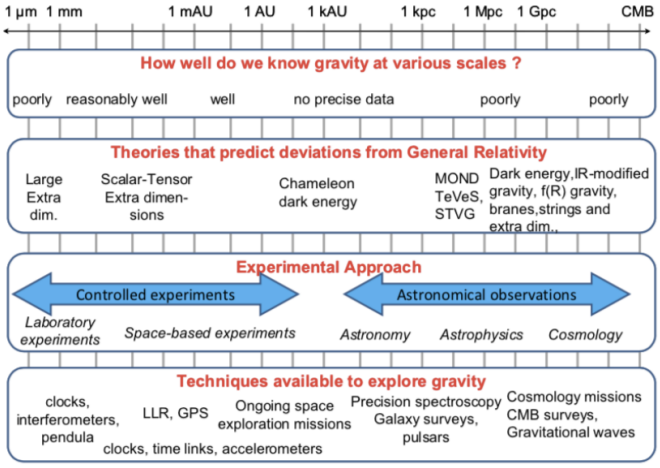

Figure 1: Knowledge of gravity at different scales (adapted from [9])

An Interstellar Probe (ISP) mission concept [2] is expected to travel faster and further than any preceding spacecraft (7 AU/year) building upon the heritage of Voyager and Pioneer missions to explore our galactic 'neighbourhood' via a suite of instruments. Its spin-stabilisation and favourable X-band antenna aperture curtail the need for re-orientation manoeuvres, enabling accurate temporal resolution of non-gravitational signals (the main source of dynamical noise in such experiments).

Email address: michaelkimon.plumaris@uniroma1.it (Michael Plumaris)

In light of these arguments, this represents an unique dynamical framework to conduct the aforementioned gravity tests. The aim of this work is to simulate this experiment by means of a covariance analysis that processes over 10 years of radiometric tracking from ground.

The first part of the experiment concerns the comparison and classification of alternative metric theories of gravity, for which we adopt the Parametrized Post Newtonian (PPN) formalism [10]. This expresses the Einstein field equations in terms of small deviations from Newton's laws, quantified by a set of parameters which take specific values in each theory. We set out to measure the Nordtvedt parameter η, searching for possible violations of the Strong Equivalence Principle (SEP), which encompasses the principle that all celestial bodies fall irrespective of their gravitational self-energy [1]. Given that η may be expanded as a combination of PPN terms, we also estimate the Eddington parameters β and γ. These express the non-linearity in the superposition law for gravity and the space-time curvature produced by a unit rest mass, respectively [11]. By definition, in GR both parameters are equal to 1 in while η is 0.

The second part of the experiment addresses scalar–tensor modifications of GR, many of which suggest a coupling between the scalar field and matter [6]. This coupling can be expressed by the Compton wavelength λ_C of the massive graviton in the Yukawa form. Its effect would be that of a "fifth force" violating the $1/r^2$ law at macroscopic scales.
This paper is structured as follows. Section 2 summarises the methodology. Section 3 describes the dynamical model, followed by the observation model in Section 4. Results and their implications are discussed in Section 5, and a conclusion is drawn in Section 6.

2. Methodology

An extensive set of numerical simulations have been conducted to address the estimation accuracy , with the underlying methodological principle being that of *precise orbit determination* (POD) [12]. This is accomplished through the processing of tracking data that allow adjusting the dynamical force models. The *a priori* dynamical model is used to retrieve a first-guess trajectory and the associated *computed* observables. The POD least-squares filter estimates of the parameters of interest by minimizing the discrepancies (residuals) between the *true* and the *computed* observables.

Given the preliminary nature of the experiment, true observables are not available. Hence a full estimation via simulated observables would result in a random realisation of the probability distribution defined by the covariance, unless dynamical model errors or non-Gaussian noise are introduced -yet these would be unrealistic as the mission design is not finalised. Moreover, a full estimation would entail the re-integration of the variational equations at each iteration, which is not ideal considering the long mission duration. To this end a *covariance analysis* is performed, mapping the uncertainty of the radiometric observables to an *uncertainty* in the sought parameters (so-called formal errors σ_i) without actually estimating their values. σ_i are obtained from the diagonal of the covariance matrix $\boldsymbol{P}$:

$$\begin{aligned} \boldsymbol{P} &= \left(\boldsymbol{P}_{apr.}^{-1} + \boldsymbol{H}^{\mathrm{T}}\boldsymbol{W}\boldsymbol{H}\right)^{-1} \\ \sigma_i &= \sqrt{\boldsymbol{P}_{ii}} \end{aligned} \tag{1}$$

with $\boldsymbol{H}$ the design matrix, describing the parameters' influence on the observables via the spacecraft dynamics, $\boldsymbol{P}_{apr.}$ the a priori covariance matrix and $\boldsymbol{W}$ the weight matrix for uncorrelated measurements.

The main accelerations are modelled in a similar fashion to the POD of the Pioneer spacecraft [13], the only "predecessors" to the ISP. In principle, one could implement complicated engineering models to predict even the slightest accelerations, yet this time-consuming process would likely yield unrealistic results. Instead, we opt for an empirical approach based on a stochastic modelling with conservative a-priori uncertainties, introduced with $\boldsymbol{P}_{apr.}$. During the actual mission, secondary measurements (temperature sensors, dust impact analysers,...) will help restricting the a-priori for a more refined POD. The figure of merit representing the POD attainable accuracy is the formal uncertainty of the three-directional constant accelerations (from Table 2):

$$\sigma_{boresight} \sim 10^{-11} m/s^2 \quad ; \quad \sigma_{other} \sim 10^{-10} m/s^2 \tag{2}$$

provided that no systematics are present, these uncertainties tend to zero as time progresses, yielding overly-optimistic results. To prevent this, a *multi-arc* approach is followed, sectioning the trajectory into 1-year arcs. This entails 10 sets of *local* parameters, namely the ISP states at the beginning of each arc and force model values, and a single set of *global* parameters, mainly the GR values affecting all arcs.

It should be noted that precision GR tests in space with LISA (Pathfinder) [14] and MICROSCOPE [15] implement a drag-free configuration, whereby the proof-mass is made to follow the geodesic trajectory. Interplanetary probes such as Bepi-Colombo or JUICE carry accelerometers [16, 17] for direct characterisation of non-gravitational forces. Nonetheless, in the present case, no mechanical instruments could withstand the 50-year planned mission duration, hence one must rely solely on the radiometric observables.

Finally, a single reference trajectory was adopted for the experiment, consisting of the baseline proposed by NASA [19]. Launching in 2036, following a Jupiter gravity assist in 2037, the ISP reaches maximum velocity, crossing the "Interstellar Boundary Explorer" ribbon at (-180°E, -22°S, 100 AU) after approximately 14.8 years. The spacecraft dynamical model was implemented in a trajectory-correction algorithm that satisfies the above boundary conditions, resulting in the hyperbolic trajectory plotted in Figure 2. The simulations have been conducted using the NASA-JPL MONTE orbit determination software library [20]. The equations of motion are integrated using a variable-step, variable-order numerical integrator [21]. The positions of the planets and moons are obtained from DE438 planetary ephemerides [22]. Light propagation is correct to order c^{-2} [23].

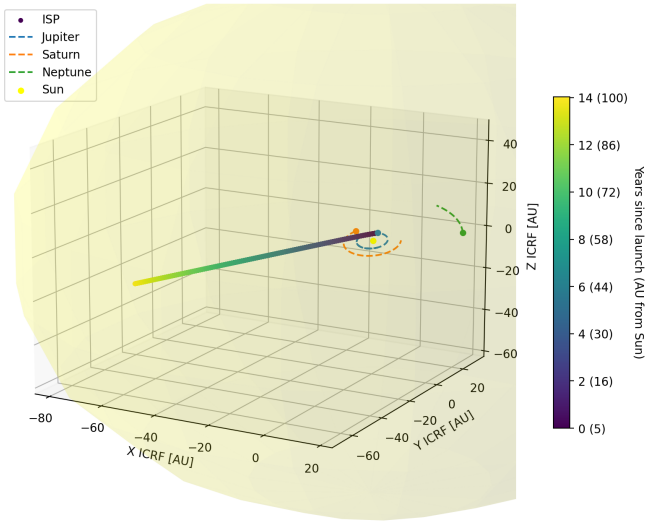

Figure 2: Interstellar Probe baseline trajectory. The shaded area represents the crossing of the helipsphere/heliosheath into the heliopause (120-200 AU [18])

3. Dynamical Model

Figure 3 depicts the main forces acting on the ISP: gravity (magnitude $\sim 10^{-5}$m/s^2), anisotropic thermal re-radiation by the Radioisotope Thermoelectric Generators (RTGs) ($\sim 10^{-9}$m/s^2), solar radiation pressure (SRP) ($\sim 10^{-10}$m/s^2 at 10 AU, decaying with r^2), and interstellar dust drag ($\sim 10^{-15}$m/s^2). The radiation pressure from the HGA transmission [24], equal to $2 \cdot 10^{-10}$m/s^2, is only present during the brief communication periods. Charged-particle effects have not been investigated as little is known on the spacecraft's potential charge during flight [25].

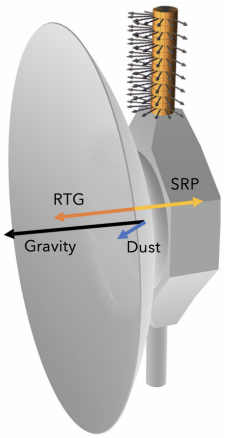

Figure 3: Representation of forces acting on the ISP.

3.1. Graviton Compton wavelength detection

In the simplest form of the massive graviton scenario, the Newtonian potential is multiplied by a Yukawa term [26]:

$$U = -G \sum_{i \neq j} \frac{m_i m_j}{r_{ij}} e^{-r_{ij}/\lambda_C} \tag{3}$$

where r_{ij} is the distance between the bodies i and j. Thus, the effect of λ_C will become more pronounced as the test body travels further from the attracting body. A reasonable approximation is to solely consider the Yukawa contribution of the Sun. We also include the Newtonian gravity of major planets, and estimate their orbits which are currently affected by uncertainties at the 100-m level [27]. To date, various methods have been used to placed lower bounds on λ_C (or, equivalently, upper limits to the graviton mass $m_g = h/c\lambda_C$). Ref. [11] argued that, if the graviton is massive, gravitational waves would travel slower in accordance with their wavelength. Consequently, the LIGO and Virgo detectors would sense this distortion of wavefronts. Cataloguing a series of gravitational wave events, [5] have reached a lower bound of $7.1 \cdot 10^{13}$ km. A similar value has been obtained via the observation of galaxy clusters [28]. Ref. [4] have placed a competitive bound of $3.9 \cdot 10^{13}$ km by dynamical fitting of INPOP (19a) ephemerides. Concerning future missions, [29, 30] infer upper limits to λ_C by a joint analysis of multiple planetary probes, whereas [31] estimate a limit of $3 \cdot 10^{16}$ km attainable with space-based detector LISA.

3.2. Testing the Equivalence Principle

A hypothetical violation of the EP is investigated by monitoring the free fall of massive bodies. A possible non-universality of the free fall should be ascribed to some coupling between gravity and the other fundamental interactions. The violation (i.e. the ratio between gravitational and inertial masses) is in general parametrised in terms of the grvaitational binding energy . In other words, the trajectories could be dependent on the chemical composition or the atomic structure of the test masses, resulting in a relative acceleration δa. In its weak form (WEP) this states that $\delta a = 0$, which has been verified to be valid at the $\delta a/a \approx 10^{-15}$ level [32].
A violation of the strong form (SEP) would indicate a coupling of the gravitation with itself. In this case, the equations of motion of body i belonging to a n-bodies system, become

$$m_i^I \mathbf{a}_i = G \sum_{j \neq i} \frac{m_i^G m_j^G}{r_{ij}^3} \mathbf{r}_{ij}; \qquad i = 1, ..., n \tag{4}$$

where the apex "I" and "G" indicate inertial and gravitational mass, respectively. The SEP violation is parametrised by

$$m_i^G / m_i^I = (1 + \eta\, \Omega_i) \tag{5}$$

where Ω_i is the ratio between self-gravitational and rest energy of body i. Since $||\Omega|| \approx 10^{-27}$ for typical spaecraft, this kind of test necessarily involves the free-fall of celestial bodies. The free-fall of the Earth and Moon towards the Sun yields a signal violation $\Omega_{Earth} = -4.4 \cdot 10^{-10}$, which is well-suited for Lunar Laser Ranging (LLR) tests that have reached an accuracy on $\delta a/a$ at the $5 \cdot 10^{-14}$ level [3]. As the present accuracy on the WEP is a factor 10 smaller [32], the parameter η can be directly constrained from LLR results, with a $\approx 10^{-4}$ level of accuracy

(when the WEP accuracy was 10^{-13}, in order to estimate η, it was necessary to combine the results of both experiments).
In our experiment, the ISP represents a quasi-inertial 'external' frame monitoring the free-fall of the Earth towards the Sun. The observed signal is proportional to $\Omega_{Sun} = -3.52 \cdot 10^{-6} \approx 10^4\,\Omega_{Earth}$. Therefore, to get a competitive bound on η, an accuracy on $\delta a/a \approx 10^{-11} - 10^{-10}$ is required.

Interestingly, η may also be estimated indirectly via a combination of PPN parameters (for details see [1]) primarily γ and β, which are thus appended as estimated parameters. Aside from its dynamical influence through η, γ induces a variation of the Shapiro delay for signals in the vicinity of a massive body. Cassini's Doppler tracking data during a Solar conjunction was processed to obtain an uncertainty for γ-1 equal to $2.3 \cdot 10^{-5}$ [33], which is likely to be improved by BepiColombo in the coming years [34]. Using this value a priori, β-1 was constrained to $3.9 \cdot 10^{-5}$ from its influence the perihelion advance of Mercury, by means of the MESSENGER spacecraft ranging data [35].

3.3. Anisotropic RTG thermal re-radiation

The spacecraft will generate forces as thermal radiation is emitted from its surfaces in an anisotropic manner, primarily originating from the RTGs. Its build up is quite significant over long timescales; had it not been for corrective maneuvers, New Horizons would have missed its Pluto encounter by 185 000 km [36]. This effect is now widely believed to be the culprit for the intriguing 'Pioneer Anomaly' detected from the Doppler tracking data of the Pioneer 10&11 spacecraft [13].

In accordance with energy conservation, the power radiated by the RTGs is equal to the heat rate produced by the decay of plutonium minus the fraction converted to electrical power (including internal ohmic losses). The re-radiation off the spacecraft body is computed using the pyRTX[1] non-gravitational accelerations computation library. Ray tracing is used to map the infrared radiation emitted from the RTGs. The antenna is the main contributor to this reflection, which induces a deceleration along the boresight direction which agrees with [36][2]. In contrast with New Horizons, here residual torques are very small ($10^{-16} m/s^2$) due to the symmetry of the RTGs. Nonetheless, due to the protracted mission duration, material degradation is expected to take place, which will vary the thermo-optical coefficients of the insulating material. Hence these are included as stochastic parameters in the estimation filter. Due to the distinguished temporal signature of this acceleration, it is accurately resolved to 1/1000 of its magnitude.

3.4. Interstellar Dust Drag

The spacecraft will experience a drag force arising from the presence of interstellar dust particles. The dust density models of [37] have been adopted to simulate these impacts. The force direction is nearly constant, as it s driven by the motion of the Solar System in the interstellar medium ($\approx$ 26 km/s). The flux of the largest particles dominates the drag calculation, yet the distribution of such particles along the trajectory is loosely constrained. During flight, this limitation will be partly overcome by in-situ measurements. As a result of its small magnitude, the dust drag will be absorbed by the estimated constant accelerations, along with the non-RTG radiation emissions and other minor effects.

3.5. Precession maneuvers

Communicating at several AU requires precise ($\leqslant 0.2^\circ$) orientation of the 5m X-band High Gain Antenna (HGA) towards Earth to maintain downlink telemetry rates. There will be static misalignments of the HGA to the principal moment of inertia (coning) as well as an Earth drift in the inertial frame. These must be corrected by precession maneuvers, that will induce nutations [38] whose damping is delayed by the long wire booms. Such maneuvers degrade the quality of the orbital estimation, as they break the "coherence" of the POD filter.

Ref. [39] predict the frequency of precession maneuvers to be roughly once per 3 days until 50 AU and decreasing after that. The reference trajectory spans from 5 to 100 AU. To reflect the fact that many parameters affecting the manoeuvre rate are still being optimised, a best-case and worst-case scenario are simulated, with maneuvers taking place once per month and once per week, respectively. These are estimated with a residual thrust uncertainty in the HGA plane.

4. Observation Model

The onboard telecommunication system will relay telemetry to ground, and determine the quality of the radiometric observables simulated in the experiment. This consists of a 5m X-Band HGA using 52W of transmitting power [38], mostly heritage from New Horizons. In the following we describe the ranging measurement process, define the tracking schedule, and compute the expected measurement noise.

4.1. Regenerative ranging

In contrast to most interplanetary missions, whereby Doppler is the main observable, here the majority of the information is cast in range measurements, as these are more sensitive to the slowly-varying dynamics [40] experienced in interstellar space.

Deep-space ranging is fundamentally a measurement of phase delay. For a two-way configuration, the ranging instrumentation measures the round-trip phase delay of the signal, propagated from the station, to the spacecraft, and back. For a three-way configuration, the signal propagates from the transmitting station, to the spacecraft, to *a different* receiving station. The measured phase values apply to a common instant in time, an epoch of the 1-pulse per second timing reference of the station clock(s) [41]. Due to the clock periodicity, this introduces a measurement ambiguity which is resolved by correlating the incoming signal with special sequence.

Modern interplanetary spacecraft operate Pseudo-Noise (PN) ranging sequences, modulating the carrier with a logical combination of the so-called range clock-sequence and several PN

[1] https://github.com/gaelccc/pyRTX
[2] https://github.com/kimonito98/InterstellarProbeRTGAcceleration/blob/174e60a1719a75b5a429752c7686d5097b94825c/RTGaccel.pdf

codes [42]. PN ranging may occur in simple turnaround or in regenerative mode. In the former, the on-board transponder performs a de/re-modulation of the carrier only. In the latter, the transponder employs a delay-locked loop to track the uplink ranging signal and regenerate a low-noise replica for downlink [41]. This technique was first demonstrated by New Horizons [43], as it offers the distinct advantage of creating a relatively noise-free copy of the uplink signal for modulation onto the downlink carrier, which is particularly important for deep-space applications. In fact, the path loss of regenerative ranging (influencing the thermal jitter, see Section 4.3) is proportional to $1/r^2$, as opposed to $1/r^4$ for transparent ranging. The downside is that the transponder must lock to the bits (chips) of the sequence and then correlate the components, incurring greater complexity on the transponder (for a comprehensive trade-off, please consult [44]).

Since the range changes significantly over the course of the signal travel time, the round-trip phase delay is processed as part of the orbital solution (in a relativistic setting) to determine the Round Trip Light Time (RTLT), subsequently used to estimate the range as a function of time.s Nonetheless, due to the three-way mode implied by the large RTLT, it requires careful consideration of station clock offsets (see Section 4.3) and estimation of multiple station biases.

4.2. Measurement Campaign

During the first 10 years the ISP will be tracked by the DSN with three 8h passes a week [19]. Based on the visibility windows in Figure 4, and the south-ecliptic nature of the baseline trajectory (see Figure 2), uplink from the DSN complex at Canberra (Australia) would maximise the elevation therefore limiting atmospheric disturbances. The measurement campaign is as follows:

- 2-way range and Doppler with Canberra until 2040;
- 3-way range and Doppler with Canberra (Up) & Madrid (Down) until 2044;
- 3-way range and Doppler with Canberra (Up) & Goldstone (Down) until 2047;
- Delta Differential One-way Ranging (angular position wrt quasar reference source) once per week.

The duration of the nominal experiment is 10 years, after which tracking will occur via the next-generation Very Large Array (ngVLA) [38]. This will involve antenna arraying, as done for the VLA and Goldstone during Voyager's encounter with Neptune [45]. Although the ngVLA will feature enhanced signal capabilities, PN ranging noise levels are difficult to predict. Hence, for the extended 20 year experiment, DSN performances are conservatively assumed.

4.3. Ranging error budget

Various sources contribute to the randomic noise component of ranging measurements. For two-way mode, the dominant contribution is thermal jitter, which is present in both in uplink and downlink -solar plasma is absent due to the southern ecliptic latitude of the baseline trajectory. Although for regenerative ranging the noise on the uplink signal is not directly modulated onto the downlink, a very small portion is carried over due to the finite bandwidth of the tracking loop. Table 1 reports this contribution for both uplink and donwlink, which may occur with a single 34m antenna or an array of 4. The latter, requiring an upgrade of DSN capabilities in terms of electronically synchronized collectors, offers an improved SNR as well as operability, flexibility and cost benefits [45]. The overall SNR values are challenging, however, if enough measurements are collected, plurality voting may be used (particularly for resolving the range ambiguity) as done for New Horizons when the spacecraft travelled beyond 22 AU and the value of $T \cdot Pr/N0$ was below 30 dB [46].

Table 1: Link budget for PN ranging at 70 AU, for integration time T = 300s. $Pr/N0$ is ranging signal power-to-noise ratio. Additional values adopted from New Horizons[47]: 1.035MHz ranging clock frequency, 0.5 modulation index, 0.25 Hz loop bandwidth, 0.9544 cross-correlation factor [41].

Component	**Uplink 34m**	**Downlink 34m**	**Downlink 4x34m**
Carrier f [GHz]	7.18	8.4	8.4
TX Power [W]	5000	52	52
TX Gain [dB]	65	50	50
EIRP [dBmi]	132	97	97
Path Loss [dB]	310	311	311
RX Gain [dBi]	49	67	74
T·Pr/N0 [dB]	59	40	47
Thermal jitter [cm]	17	18	8

For three-way mode, one must also take into account the error induced by the desyncronisation between the two ground stations. Although coherent transposition of the signal does not rely on an onboard frequency reference (no atomic clock could operate for 50 years anyways), the precise ground transmission and reception times are needed to correlate the signal. For present purposes the Station Time (ST) is especially significant. This is an atomic time generated at the ground station showing slight deviations from the reference time (UTC). For the case of 2-way ranging (i.e. same uplink and downlink station), the relevant quantity is the ST stability: DSN H-masers can guarantee a stability of $\sim 10^{-15}$ over a day [48], meaning the clock noise contribution to ranging noise is negligible. For 3-way mode, however, one must correct for ST offsets between participating stations. Synchronisation at intercontinental distances (here between two ground stations) is accomplished using "all-in-view" GPS time transfer technique, which is nowadays capable of ns-level accuracy [49], corresponding to 30cm of range error.

Additionally, there is always some delay between the onboard reception of a signal at the front end of the HGA and the retransmission from the HGA, mainly due to processing in the onboard electronics [50]. In line with modern transponders such as BepiColombo's KaT [51], which are endowed with an onboard calibration system, the residual uncalibrated delay is only a few cm.

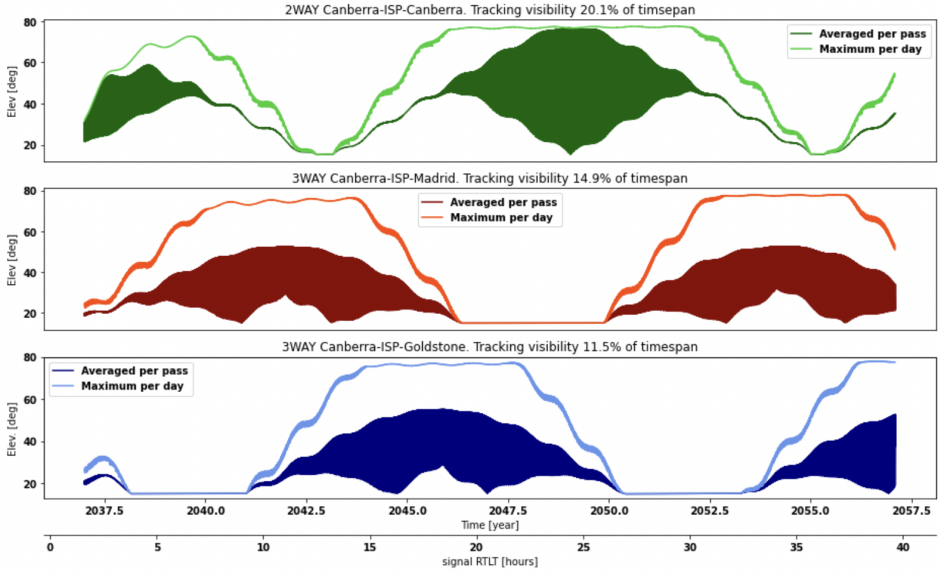

Figure 4: ISP elevations per DSN complex. Canberra selected for uplink to curtail atmospheric delays. Elevation cutoff set to 15°.

The assessment of range error systematics is more complex, primarily due to the difficulty in separating media effects from station biases [52], requiring their inclusion in the estimation filter. These arise from ionospheric and -wet- tropospheric effects. For an optimistic and pessimistic bound, station biases of 30 cm are assumed stable for 1 month, as well as every week (BepiColombo experiments assume a stability $\geqslant$2 weeks, personal communication) and estimated as stochastic parameters in the filter.

In light of the above discussion, to cover a wide set of cases, range data are simulated as having a random noise contribution of 1m or 30cm, at 300s integration time. These values are in agreement with 2-way PN regenerative ranging residuals for New Horizons [47].

5. Results & Discussion

The orbit determination filter processes $\approx$ 480 000 observables to solve for 990 up to 3386 local parameters (depending on the bias stability and manoeuvre frequency) for each 1-year arc, and 12 global parameters, as reported in Table 2. For the relativistic parameters, the formal uncertainties are compared to their a-priori knowledge to obtain the 'Improvement Factor' plotted in Figure 5, whereby the various mission cases are distinguished by the color bars. To reflect on the influence of GR deviations on our setup as compared to the 'typical' case of planetary orbiters, Figure 6 displays the partial derivatives of the ISP (left) and the Earth (right) states with respect to the parameters, multiplied by their current a-priori knowledge.

Focusing on Figure 5, evidently, no improvement is expected for β and γ. This is also reflected by the y-scales in Figure 6, which indicate a stronger signal in the planetary case. In fact, a much better estimate will be obtained by BepiColombo [34], which disposes of a dual-band transponder (X & Ka) to calibrate the plasma dispersion during solar conjunctions (when the signal is strongest)

Table 2: Covariance analysis results. Local parameters (top half) are estimated pa = per arc, pm = per month, pw = per week. The '$\sim$' symbols distinguish the best and worst value.

Parameter Name	**A priori value**	**Formal Error**
Spacecraft pos.	100m (x3)	10m rms pa
Spacecraft vel.	1m/s (x3)	1-0.1mm/s rms pa
Solar Pres. cf	0.1 inter-month	0.01$\sim$0.03 pm
Constant acc.	none	$10^{-10} \sim 10^{-11}$ m/s rms pa
RTG radiation	10^{-9}m/s^2 (x3)	$10^{-10} \sim 10^{-12}$ m/s rms pa
Thruster misal.	1 mm/s (x2)	0.1 $\sim$ 0.001 rms pw/pm
Range bias	30cm	stochastic
Sun GM	0.4 km^3/s^2 [53]	no improvement
Sun J_2	$2 \cdot 10^{-8}$ [53]	no improvement
Earth state	50m [27]	20$\sim$40m
γ-1	$2.3 \cdot 10^{-5}$ [33]	no improvement
β-1	$3.9 \cdot 10^{-5}$ [35]	no improvement
η	$1.1 \cdot 10^{-4}$ [3]	$1.5 \cdot 10^{-5} \sim 8.9 \cdot 10^{-5}$
λ_C	$7.1 \cdot 10^{13}$km [5]	$1.4 \cdot 10^{14} \sim 7.2 \cdot 10^{13}$km

A significant breakthrough is projected for η, enhanced by a factor 2 in most cases, and up to a factor 7 in the best scenario, corresponding to a formal uncertainty of $1.5 \cdot 10^{-5}$. Although the influence of η is much stronger for the Earth case (see the y-scale in Figure 6), ranging measurements benefit from the *combined* "signature" since the ISP acts as a quasi-inertial frame observing the Earth's fall into the Sun's gravitational field. For this same reason, one also finds an accompanying improvement in the knowledge for the Earth position in the inertial frame. Taking the best scenario and extending the experiment to 20 years yields a formal error $\leqslant 10^{-6}$. This estimate would serve to (dis)prove the universality of the free fall for bodies with a

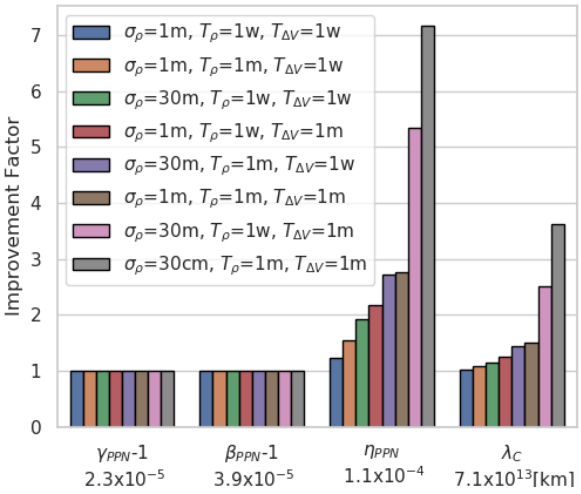

Figure 5: Improvement factor wrt a-priori uncertainty of sought parameters. Mission cases are distinguished by ranging accuracy (σ_ρ), ranging bias stability (T_ρ) and precession manoeuvre frequency ($T_{\Delta V}$). m = month, w = week.

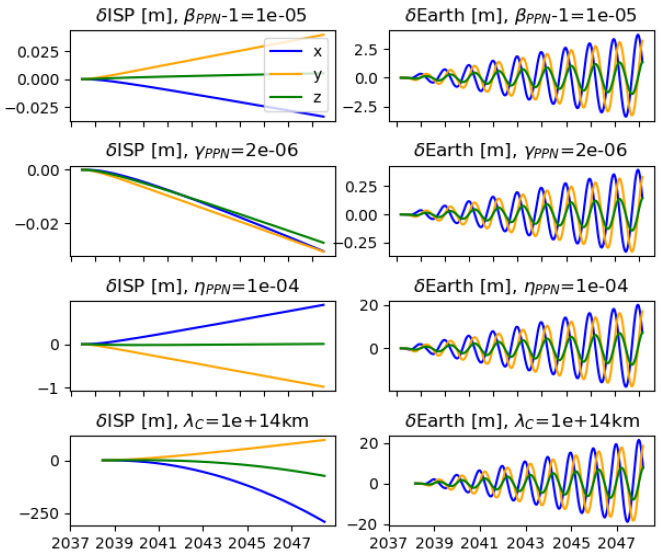

Figure 6: Amplitude of deviation in the ISP (left) & Earth (right) states with respect to parameters of interest, multiplied by the reference values (BepiColombo-projected values for β and γ [23]). Note: coordinates in ICRF as for Figure 2

non-negligible self-gravitational energy.

The parameter λ_C also displays a promising estimation accuracy, with the best two cases surpassing the 10^{14}km bound. In contrast to η, the majority of the signal affects the ISP state directly, given that λ_C inflicts a signature which increases exponentially with the distance to the Sun (see Equation 3). For a 20 year experiment, the uncertainty reaches a value of $\approx 10^{15}$km, and extending the experiment further to 30 years (with sparser ranging data) would strengthen this bound to beyond 10^{16}km. This parameter tests the validity of the $1/r^2$ law at unprecedented accuracies, or potentially suggests a coupling of matter by demonstrating that the graviton does indeed hold a mass.

Looking at Figure 6, in the Earth -or equivalently the planetary orbiter- case, the signals of β, γ, η and λ_C are of secular and/or periodic nature, with planar components almost indistinguishable. On the other hand, the ISP signals inflict a more distinct signature, manifested as an initial 'kick' which deviates the trajectory over time. These steady-state dynamics stress the importance of accurate and continuous ranging measurements in the prospect of future GR tests.

Overall, the tallest violet bar indicates that, *ceteris paribus*, a low frequency for precession maneuvers is desirable over a long stability for the ground station bias. Whereas the former is influenced primarily by the moment of inertia around the boresight direction, the latter depends on the quality of ground station delay and atmospheric calibrations [8]. The system design should aim to limit these maneuvers, or, equivalently, ranging data should be collected in deep space ($\geqslant$ 50AU) when their necessity is at its lowest.

6. Conclusion

We have carried out a covariance analysis to grasp the estimation accuracy for a series of parameters associated with GR, by simulating 10 years of radiometric data from the ISP mission concept. These parameters are part of the PPN formalism, which enables comparison and classification of alternative metric theories of gravity [1]. The methodology rests on the assumption that DSN stations will perform clock synchronisation to the ns-level to enable accurate 3-way PN ranging observables, as well as a mission design that minimises the antenna repointing maneuvers, which have a detrimental effect on the estimation process.

The present results highlight the unique opportunity the ISP has in testing the validity of GR by estimating η and λ_C. The former is estimated to less than 10^{-4} for all mission cases, whereas the latter surpasses the 10^{14}km lower margin for the two best scenarios. The ISP provides an opportunity to test the $1/r^2$ law at distances where the laws of gravity have never been precisely measured. The nominal tracking experiment we have considered lasts 10 years. Nonetheless, extending the time span of the measurements beyond 10 years would further tighten the uncertainty on the parameters, especially for λ_C which inflicts an exponential signature on the spacecraft range.

Acknowledgements. The authors would like to thank Gabe Rogers and Ralph McNutt, responsible for the ISP development at JHUALP, for the insightful discussions at COSPAR 2022. The authors are also grateful to Silvan Hunziker and Veerle Sterken for their support in modelling the dust impacts. The authors acknowledge the support from NASA under the grant no. 80GSFC21M0002.

References

[1] C. M. Will, The confrontation between general relativity and experiment, Living Reviews in Relativity 9 (1) (jun 2014). doi:10.12942/lrr-2014-4.

[2] R. L. McNutt, R. F. Wimmer-Schweingruber, M. Gruntman, S. M. Krimigis, E. C. Roelof, P. C. Brandt, S. R. Vernon, M. V. Paul, et al., Interstellar probe – destination: Universe!, Acta Astronautica 196 (2022) 13–28. doi:https://doi.org/10.1016/j.actaastro.2022.04.001.

[3] F. Hofmann, J. Müller, Relativistic tests with lunar laser ranging, Classical and Quantum Gravity 35 (02 2018). doi:10.1088/1361-6382/aa8f7a.

[4] L. Bernus, O. Minazzoli, A. Fienga, M. Gastineau, J. Laskar, et al., Constraint on the yukawa suppression of the Newtonian potential from the planetary ephemeris inpop19a, Physical Review D 102 (2) (Jul 2020). doi:10.1103/physrevd.102.021501.

[5] R. Abbott, T. Abbott, S. Abraham, F. Acernese, K. Ackley, et al., Tests of general relativity with binary black holes from the second LIGO-Virgo gravitational-wave transient catalog, Physical Review D 103 (12) (Jun 2021). doi:10.1103/physrevd.103.122002.

[6] T. Damour, Theoretical aspects of the equivalence principle, Classical and Quantum Gravity 29 (18) (2012) 184001. doi:10.1088/0264-9381/29/18/184001.

[7] B. P. Abbott, R. Abbott, T. Abbott, M. Abernathy, F. Acernese, et al., Observation of gravitational waves from a binary black hole merger, Physical review letters 116 (6) (2016) 061102.

[8] P. Cappuccio, V. Notaro, A. di Ruscio, L. Iess, A. Genova, et al., Report on first inflight data of BepiColombo's Mercury orbiter radio science experiment, IEEE Transactions on Aerospace and Electronic Systems 56 (6) (2020) 4984–4988. doi:10.1109/TAES.2020.3008577.

[9] S. G. Turyshev, Experimental tests of general relativity: recent progress and future directions, Physics-Uspekhi 52 (1) (2009) 1–27. doi:10.3367/ufne.0179.200901a.0003.

[10] C. M. Will, K. Nordtvedt, Jr., Conservation Laws and Preferred Frames in Relativistic Gravity. I. Preferred-Frame Theories and an Extended PPN Formalism, Astrophys. J. 177 (1972) 757. doi:10.1086/151754.

[11] C. M. Will, Bounding the mass of the graviton using gravitational-wave observations of inspiralling compact binaries, Phys. Rev. D 57 (1998) 2061–2068. doi:10.1103/PhysRevD.57.2061.

[12] O. Montenbruck, E. Gill, Satellite Orbits: Models, Methods, and Applications, Physics and astronomy online library, Springer Berlin Heidelberg, 2000.

[13] J. D. Anderson, P. A. Laing, E. L. Lau, A. S. Liu, M. M. Nieto, S. G. Turyshev, Study of the anomalous acceleration of Pioneer 10 and 11, Physical Review D 65 (8) (apr 2002). doi:10.1103/physrevd.65.082004.

[14] M. Armano, et al., Beyond the required LISA free-fall performance: New LISA pathfinder results down to 20μHz, Phys. Rev. Lett. 120 (2018) 061101. doi:10.1103/PhysRevLett.120.061101.

[15] P. Touboul, G. Métris, V. Lebat, A. Robert, The microscope experiment, ready for the in-orbit test of the equivalence principle, Classical and Quantum Gravity 29 (18) (2012) 184010. doi:10.1088/0264-9381/29/18/184010.
URL https://dx.doi.org/10.1088/0264-9381/29/18/184010

[16] V. Iafolla, E. Fiorenza, C. Lefevre, A. Morbidini, S. Nozzoli, R. Peron, M. Persichini, A. Reale, F. Santoli, Italian Spring Accelerometer (ISA): A fundamental support to BepiColombo Radio Science Experiments, Planet. Space Sci. 58 (2010) 300–308. doi:10.1016/j.pss.2009.04.005.

[17] D. Lucchesi, V. Iafolla, The Non-Gravitational Perturbations impact on the BepiColombo Radio Science Experiment and the key role of the ISA accelerometer: direct solar radiation and albedo effects, Celestial Mechanics and Dynamical Astronomy 96 (2006) 99–127. doi:10.1007/s10569-006-9034-9.

[18] D. B. Reisenfeld, M. Bzowski, H. O. Funsten, J. Heerikhuisen, P. H. Janzen, M. A. Kubiak, D. J. McComas, N. A. Schwadron, J. M. Sokół, A. Zimorino, E. J. Zirnstein, A three-dimensional map of the heliosphere from ibex, The Astrophysical Journal Supplement Series 254 (2) (2021) 40. doi:10.3847/1538-4365/abf658.
URL https://dx.doi.org/10.3847/1538-4365/abf658

[19] R. L. McNutt, et al., Interstellar Probe: NASA Solar and Space Physics Mission Concept Study, JHUALP, 2021.

[20] S. Evans, W. Taber, T. Drain, J. Smith, H.-C. Wu, M. Guevara, R. Sunseri, J. Evans, Monte: the next generation of mission design and navigation software, CEAS Space Journal 10 (2018) 79–86.

[21] S. Evans, W. Taber, T. Drain, J. Smith, H.-C. Wu, M. Guevara, R. Sunseri, J. Evans, Monte: the next generation of mission design and navigation software, CEAS Space Journal 10 (01 2018). doi:10.1007/s12567-017-0171-7.

[22] W. M. Folkner, R. S. Park, Planetary ephemeris DE438 for Juno, JPL Inter-Office Memorandum (2018).

[23] P. Cappuccio, I. di Stefano, G. Cascioli, L. Iess, Comparison of light-time formulations in the post-Newtonian framework for the bepicolombo more experiment, Classsbncal and Quantum Gravity 38 (2021) 227001. doi:10.1088/1361-6382/ac2b0a.

[24] S. G. Turyshev, V. T. Toth, The pioneer anomaly, Living Reviews in Relativity 13 (2010) 1–175.

[25] G. Afonso, F. Barlier, C. Berger, F. Mignard, J. J. Walch, Reassessment of the charge and neutral drag of LAGEOS and its geophysical implications, Journal of Geophysical Research: Solid Earth 90 (B11) (1985) 9381–9398. doi:https://doi.org/10.1029/JB090iB11p09381.

[26] C. M. Will, Solar system versus gravitational-wave bounds on the graviton mass, Classical and Quantum Gravity 35 (17) (2018) 17LT01. doi:10.1088/1361-6382/aad13c.

[27] A. Fienga, P. Deram, A. Di Ruscio, V. Viswanathan, J. I. B. Camargo, L. Bernus, M. Gastineau, J. Laskar, INPOP21a planetary ephemerides, Notes Scientifiques et Techniques de l'Institut de Mecanique Celeste 110 (Jun. 2021).

[28] A. Piórkowska-Kurpas, S. Cao, M. Biesiada, Graviton mass from X-COP galaxy clusters, Journal of High Energy Astrophysics 33 (2022) 37–43. doi:https://doi.org/10.1016/j.jheap.2022.01.001.

[29] F. De Marchi, G. Cascioli, Testing general relativity in the solar system: present and future perspectives, Classical and Quantum Gravity 37 (05 2020). doi:10.1088/1361-6382/ab6ae0.

[30] G. Cascioli, F. D. Marchi, A. Genova, L. Iess, D. E. Smith, M. T. Zuber, The contribution of a large baseline intersatellite link to relativistic metrology, 2019 IEEE 5th International Workshop on Metrology for AeroSpace (MetroAeroSpace) (2019) 579–583doi:10.1109/MetroAeroSpace.2019.8869641.

[31] E. Berti, J. Gair, A. Sesana, Graviton mass bounds from space-based gravitational-wave observations of massive black hole populations, Phys. Rev. D 84 (2011) 101501. doi:10.1103/PhysRevD.84.101501.

[32] P. Touboul, G. Métris, M. Rodrigues, J. Bergé, otthers, Microscope mission: Final results of the test of the equivalence principle, Phys. Rev. Lett. 129 (2022) 121102. doi:10.1103/PhysRevLett.129.121102.

[33] B. Bertotti, L. Iess, P. Tortora, A test of general relativity using radio links with the cassini spacecraft, Nature 425 (2003) 374–6. doi:10.1038/nature01997.

[34] I. di Stefano, P. Cappuccio, L. Iess, The bepicolombo solar conjunction experiments revisited, Classical and Quantum Gravity 38 (5) (2020) 055002. doi:10.1088/1361-6382/abd301.

[35] R. S. Park, W. M. Folkner, A. S. Konopliv, J. G. Williams, D. E. Smith, M. T. Zuber, Precession of Mercury's perihelion from ranging to the MESSENGER spacecraft, The Astronomical Journal 153 (3) (2017) 121. doi:10.3847/1538-3881/aa5be2.

[36] G. Rogers, S. Hefter, Radioisotope thermoelectric generator effects on the dynamics of spacecraft. poster at COSPAR 44th assmbly in Athens, Greece. 16-24 july, 2022, COSPAR 44th Assembly Poster Session (07 2022).

[37] S. Hunziker, V. Sterken, P. Strub, H. Krüger, A. Li, Opportunities for interstellar dust detection by the Interstellar Probe, EPSC 2021 (2021). doi:10.5194/epsc2021-529.

[38] R. Ashtari, D. Copeland, J. Kinnison, G. Rogers, R. McNutt, Interstellar communications, in: 2021 IEEE Aerospace Conference (50100), 2021, pp. 1–10. doi:10.1109/AERO50100.2021.9438311.

[39] G. D. Rogers, J. D. Kinnison, P. C. Brandt, A. A. Cocoros, M. V. Paul, Dynamic challenges of long flexible booms on a spinning outer heliospheric spacecraft, in: 2021 IEEE Aerospace Conference (50100), 2021, pp. 1–11. doi:10.1109/AERO50100.2021.9438510.

[40] D. Dirkx, I. Prochazka, S. Bauer, P. Visser, R. Noomen, L. I. Gurvits, B. Vermeersen, Laser and radio tracking for planetary science missions—a comparison, Journal of Geodesy 93 (11) (2018) 2405–2420. doi:10.1007/s00190-018-1171-x.

[41] JPL, Telecommunications link design handbook: Pseudo-noise and regenerative ranging, JPL Inter-Office Memorandum 810-005 (2019).

[42] J. B. Berner, P. W. Kinma, J. M. Layland, Regenerative pseudo-noise ranging for deep space applications (2001).

[43] C. B. Haskins, D. J. Duven, C. C. DeBoy, J. R. Jensen, First deep-space

flight demonstration of regenerative pseudo-noise ranging, in: 2012 IEEE Aerospace Conference, 2012, pp. 1–6. doi:10.1109/AERO.2012.6187117.

[44] P. Holsters, G. Boscagli, E. Vassallo, Pseudo-noise ranging for future transparent and regenerative channels, in: SpaceOps 2008 Conference, 2008, p. 3277.

[45] D. H. Rogstad, A. Mileant, T. T. Pham, Antenna arraying techniques in the deep space network, John Wiley & Sons, 2005.

[46] J. R. Jensen, A plurality voting method for acquisition of regenerative ranging measurements, in: 2013 IEEE Aerospace Conference, IEEE, 2013, pp. 1–7.

[47] J. Jensen, C. Haskins, C. DeBoy, Regenerative pn ranging experience with New Horizons during 2012, IEEE Aerospace Conference Proceedings (2013) 1–7doi:10.1109/AERO.2013.6496983.

[48] JPL, Telecommunications link design handbook: Frequency and timing, JPL Inter-Office Memorandum 810-005 (2021).

[49] A. Bauch, Time and frequency comparisons using radiofrequency signals from satellites, Comptes Rendus Physique 16 (5) (2015) 471–479, the measurement of time / La mesure du temps. doi:https://doi.org/10.1016/j.crhy.2015.02.006.

[50] J. Border, M. Paik, Station delay calibration for ranging measurements, Interplanetary Network Progress Report (05 2009).

[51] L. Iess, S. W. Asmar, P. Cappuccio, G. Cascioli, et al., Gravity, geodesy and fundamental physics with bepicolombo's more investigation, Space Science Reviews 217 (2021) 1–39. doi:10.1007/s11214-021-00800-3.

[52] L. Iess, M. Di Benedetto, N. James, M. Mercolino, L. Simone, P. Tortora, Astra: Interdisciplinary study on enhancement of the end-to-end accuracy for spacecraft tracking techniques, Acta Astronautica 94 (2) (2014) 699–707. doi:https://doi.org/10.1016/j.actaastro.2013.06.011.

[53] A. Fienga, J. Laskar, P. Exertier, H. Manche, M. Gastineau, Numerical estimation of the sensitivity of inpop planetary ephemerides to general relativity parameters, Celestial Mechanics and Dynamical Astronomy 123 (11 2015). doi:10.1007/s10569-015-9639-y.